

# A Role for ERK MAP Kinase in Physiologic Temporal Integration in Hippocampal Area CA1

Joel C. Selcher,<sup>1</sup> Edwin J. Weeber,<sup>1</sup> Jill Christian,<sup>1</sup> Tanya Nekrasova,<sup>2</sup>  
Gary E. Landreth,<sup>2</sup> and J. David Sweatt<sup>1,3</sup>

<sup>1</sup>Division of Neuroscience, Baylor College of Medicine, Houston, Texas 77030, USA;

<sup>2</sup>Alzheimer's Research Laboratory, Case Western Reserve University School of Medicine, Cleveland, Ohio 44106, USA

Recent studies demonstrate a requirement for the Extracellular signal Regulated Kinase (ERK) mitogen-activated protein kinase (MAPK) cascade in both the induction of long-lasting forms of hippocampal synaptic plasticity and in hippocampus-dependent associative and spatial learning. In the present studies, we investigated mechanisms by which ERK might contribute to synaptic plasticity at Schaffer collateral synapses in hippocampal slices. We found that long-term potentiation (LTP) induced with a pair of 100-Hz tetani does not require ERK activation in mice whereas it does in rats. However, in mice, inhibition of ERK activation blocked LTP induced by two LTP induction paradigms that mimicked the endogenous  $\theta$  rhythm. In an additional series of studies, we found that mice specifically deficient in the ERK1 isoform of MAPK showed no impairments in tests of hippocampal physiology. To investigate ERK-dependent mechanisms operating during LTP-inducing stimulation paradigms, we monitored spike production in the cell body layer of the hippocampus during the period of  $\theta$ -like LTP-inducing stimulation.  $\theta$ -burst stimulation (TBS) produced a significant amount of postsynaptic spiking, and the likelihood of spike production increased progressively over the course of the three trains of TBS independent of any apparent increase in Excitatory Post-Synaptic Potential (EPSP) magnitude. Inhibition of ERK activation dampened this TBS-associated increase in spiking. These data indicate that, for specific patterns of stimulation, ERK may function in the regulation of neuronal excitability in hippocampal area CA1. Overall, our data indicate that the progressive increase in spiking observed during TBS represents a form of physiologic temporal integration that is dependent on ERK MAPK activity.

Although evidence from studies of hippocampal synaptic plasticity and of the behaving animal indicates that activation of protein kinases contributes to the formation of memories, the underlying signal transduction mechanisms remain largely unknown. In particular, although a variety of studies with protein kinase inhibitors demonstrate a necessity for protein kinase activation in the induction of long-term potentiation (LTP) in hippocampal area CA1, the basis for kinase inhibitors blocking LTP induction is unclear. The pluripotent nature and structural diversity of most second messenger-regulated kinases make it difficult to determine precisely which downstream targets and physiologic effects are necessary components of kinase regulation of LTP induction.

An increasing number of studies of late have investigated the role of the ERK mitogen-activated protein kinase (MAPK) cascade in hippocampal synaptic plasticity. Several laboratories have demonstrated that inhibitors of ERK MAPK activation, that is, inhibitors of the dedicated upstream regulator of ERK Mitogen and Extracellular signal

regulated Kinase (MEK), block the induction of N-Methyl-D-Aspartate (NMDA) receptor-dependent LTP. In the present studies, we sought to begin to extend these studies by investigating two aspects of ERK involvement in LTP. First, ERK comprises two isoforms, ERK1 (p44 MAPK) and ERK2 (p42 MAPK). We determined that genetic deletion of the ERK1 isoform did not diminish LTP induction at Schaffer collateral synapses. Second, we sought to increase our understanding of how it is that loss of ERK activation leads to a diminution of LTP induction. In these studies, using  $\theta$ -burst pattern stimulation, we found that TBS causes an acute increase in the likelihood of action potential firing over the course of the  $\theta$ -pattern stimulation. This increase in action potential firing, a form of temporal integration, was significantly attenuated by inhibition of ERK activation. Thus, our data indicate the hypothesis that one component of ERK inhibitor blockade of LTP induction is blockade of an ERK-dependent temporal integration mechanism controlling postsynaptic action potential firing in hippocampal pyramidal neurons.

## RESULTS

One goal of the present studies was to investigate if *ERK1*-deficient knockout mice were diminished in their capacity

<sup>3</sup>Corresponding author.

E-MAIL: [jsweatt@bcm.tmc.edu](mailto:jsweatt@bcm.tmc.edu); FAX (713) 798-3946

Article and publication are at <http://www.learnmem.org/cgi/doi/10.1101/lm.51103>.

for LTP. As all of our prior LTP studies had been performed using rats, to analyze synaptic plasticity in the mouse model system, we examined tetanus-induced hippocampal LTP of the Schaffer collateral-CA1 pyramidal cell synapse in mouse hippocampal slices. Tetanus-induced LTP is an activity-dependent form of plasticity in which brief trains of high-frequency stimulation (HFS) elicit a long-lasting increase in synaptic efficacy (Bliss and Lomo 1973). In both rats and mice, LTP is reliably induced in area CA1 of the hippocampus following a stimulation paradigm consisting of two trains of 1-s, 100-Hz tetani. A selective inhibitor of the ERK/MAPK cascade, PD098059, was recently found to block the induction of this form of LTP in the rat hippocampus (English and Sweatt 1996). In order to test whether MAPK plays an equally important role in the mouse, we evaluated the effect of inhibitors of MAPK activation on LTP in mouse hippocampal slices.

Slices were exposed to an inhibitor of MEK (20  $\mu$ M U0126), or to vehicle (0.1% dimethyl sulfoxide [DMSO]) for 1 h prior to standard LTP-inducing tetanic stimulation. Surprisingly, inhibiting MAPK activation produced no effect on LTP induced with this high-frequency tetanic stimulation (Fig. 1A; 45 min after tetanization:  $148.5 \pm 9.2\%$  of baseline for vehicle-treated slices vs.  $156.8 \pm 10.2\%$  for U0126-treated slices, respectively;  $P > 0.05$ ). Similar results were obtained using a second MEK inhibitor, SL327 (10  $\mu$ M SL327; 45 min after tetanization:  $144.0 \pm 7.3\%$  of baseline for SL327-treated slices;  $P > 0.05$ ). These findings indicate that LTP induced with a pair of 100-Hz tetani does not require ERK activation in mice. Comparing these findings with previously published results using rat hippocampus indicates the possibility that rats and mice do not use identical molecular mechanisms for the induction of this particular form of synaptic plasticity. In fact, in parallel experiments using rat hippocampal slices maintained side-by-side in the same slice chamber, and so forth, we observed a blockade of LTP induction in rat slices using the identical stimulation protocol (Fig. 1B; 45 min after tetanization:  $153.9 \pm 7.1\%$  of baseline for vehicle-treated slices vs.  $115.0 \pm 12.5\%$  and  $117.9 \pm 8.0\%$  for SL327- and U0126-treated slices, respectively;  $P < 0.0001$  for both MEK inhibitors).

To be sure that the 100-Hz protocol was not eliciting an NMDA-receptor independent form of LTP in the mouse slices, we tested as a control the effect of the NMDA antagonist Amino-Phosphono Valeric Acid (APV) on LTP induced with this high-frequency tetanic stimulation. The NMDA antagonist was applied to slices 1 h prior to stimulation, and, as expected, 50  $\mu$ M APV completely blocked LTP in both mouse and rat hippocampal slices (Fig. 2A,B; 45 min after tetanization:  $105.6 \pm 8.9\%$  [ $P < 0.0001$ ] and  $111.4 \pm 7.4\%$  [ $P < 0.0001$ ] of baseline, respectively). These findings confirm that LTP-induced with a pair of 100-Hz tetani is NMDA receptor-dependent in the mouse under our experimental conditions.

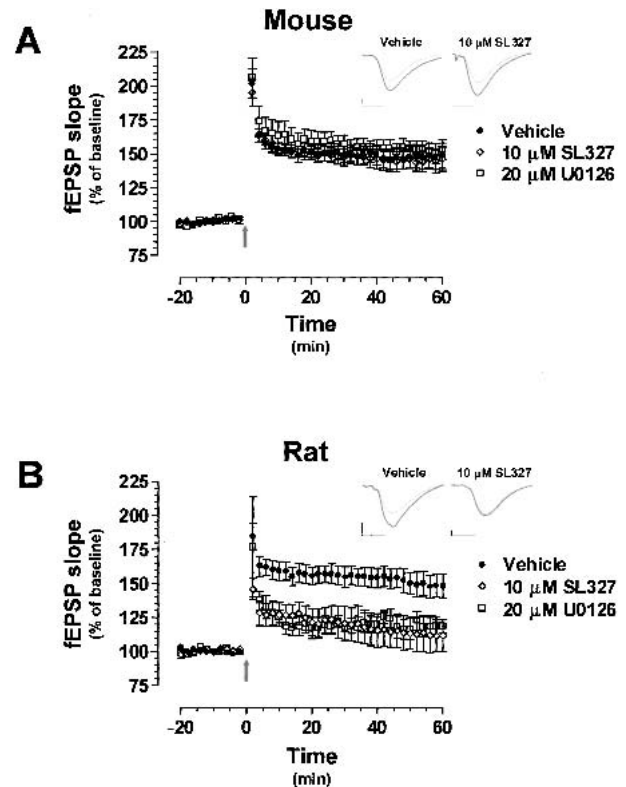


**Figure 1** 100-Hz long-term potentiation (LTP) does not require ERK activation in mouse hippocampus. (A) LTP induced with a pair of 100-Hz tetani in mouse hippocampal slices in the presence of either vehicle ( $n = 19$ ), 10  $\mu$ M SL327 ( $n = 11$ ), or 20  $\mu$ M U0126 ( $n = 10$ ). Inset, representative traces from vehicle- and SL327-treated mouse slices before (gray) and after (black) tetanization. Scale bars are 1 mV by 8 msec. (B) LTP induced with this same induction protocol in rat hippocampal slices in the presence of either vehicle ( $n = 10$ ), 10  $\mu$ M SL327 ( $n = 7$ ), or 20  $\mu$ M U0126 ( $n = 5$ ). Inset, representative traces from vehicle- and SL327-treated mouse slices before (gray) and after (black) tetanization. Scale bars are 1 mV by 8 msec. fEPSP = field Excitatory Postsynaptic Potential

We also wanted to be certain of the efficacy of the MEK inhibitor U0126 in blocking ERK activation. Therefore, the ability of U0126 to block cAMP-stimulated ERK activation was also tested. Twenty micromolar U0126 completely blocked elevation of phospho-ERK levels following treatment with 50  $\mu$ M forskolin in area CA1 of hippocampal slices prepared from mice (Fig. 3). Thus, it appears that the lack of LTP blockade by MEK inhibitors does not result from an inability of U0126 to effectively block ERK activation.

Mice are notoriously variable depending on their particular genetic background strain, and strain differences in signal transduction pathways have been reported (Paylor et al., 1996; Crawley et al. 1997). To ensure that a lack of effect of MEK inhibitors on HFS-induced LTP was not limited to a particular mouse strain, the LTP experiments were conducted with hippocampi from two additional mouse strains: another inbred strain, 129/SvImJ, and an outbred

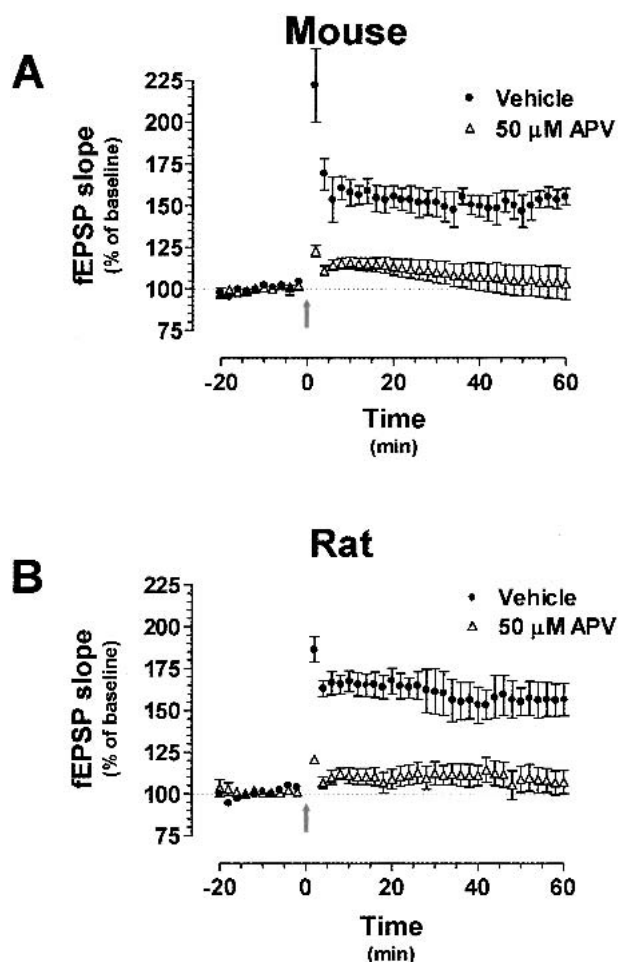


**Figure 2** 100-Hz long-term potentiation (LTP) is NMDA receptor-dependent in the mouse hippocampus. (A) LTP induced with a pair of 100-Hz tetani in the presence of either vehicle ( $n = 5$ ) or 50  $\mu\text{M}$  APV ( $n = 4$ ). High-frequency stimulation (HFS)-LTP was completely blocked by the NMDA receptor antagonist in both sets of hippocampal slices. (B) Hippocampal slices prepared from rat brains were exposed to the same LTP-induction paradigm in the presence of either vehicle ( $n = 6$ ) or 50  $\mu\text{M}$  APV ( $n = 5$ ). HFS-LTP was completely blocked by the NMDA receptor antagonist in both sets of hippocampal slices. fEPSP = field Excitatory Postsynaptic Potential

strain, CD1. As with the C57BL/6 mice, the MEK inhibitors failed to impair LTP in hippocampal slices from these mice (data not shown), indicating that this is not merely a strain effect.

### MEK Inhibition Impairs LTP Induced by Stimulation in the $\theta$ Frequency

We also tested other LTP induction protocols to determine their ERK dependence. On the basis of the potential behavioral importance of the hippocampal  $\theta$  rhythm, we decided to focus on LTP induction paradigms that mimicked this endogenous activity (Larson et al. 1986). One such para-

digm effective at producing LTP in the mouse hippocampus involves brief stimulation in the  $\theta$  frequency range. Specifically, the  $\theta$ -frequency stimulation (TFS) protocol that we used consisted of 30 sec of 5-Hz stimulation (Fig. 4A). This stimulation protocol evoked stable LTP in vehicle-treated slices (Fig. 4B; 45 min after tetanization:  $151.26 \pm 8.10\%$  of baseline). Unlike the HFS-LTP, however, blockade of ERK activation with 20  $\mu\text{M}$  U0126 significantly suppressed the induction of LTP induced with this TFS (45 min after tetanization:  $121.25 \pm 5.40\%$  of baseline;  $P < 0.001$ ).

Having shown that ERK activation contributes to LTP induced with TFS, we investigated the effect of MEK inhibition on a similar  $\theta$ -frequency-based pattern of stimulation. This stimulation protocol, known as TBS, was designed to more accurately mimic the typical firing pattern of hippocampal pyramidal neurons during  $\theta$  (Larson et al. 1986). TBS consisted of three trains of 10 pulses of four 100-Hz bursts delivered at 5 Hz with an intertrain interval of 20 sec (Fig. 5A). In response to this stimulation, vehicle-treated control slices exhibited robust LTP (Fig. 5B; 45 min after tetanization:  $157.51 \pm 7.89\%$  of baseline). In slices preexposed to U0126, however, induction of LTP was blocked, indicating a requirement for ERK activation in this form of LTP (45 min after tetanization:  $120.28 \pm 7.03\%$  of baseline;  $P < 0.0001$ ). Taken together with our previous LTP experiments, these data indicate that, in mice, ERK activation is selectively necessary for distinct forms of LTP and its involvement depends on the pattern of stimulation used to evoke LTP.

### Effects of MEK Inhibitors on Acute Changes in Action Potential Firing With LTP-Inducing Stimulation

Because of the differential sensitivity to MEK inhibition displayed by the three LTP induction protocols tested, it appeared that ERK was involved selectively in distinct forms

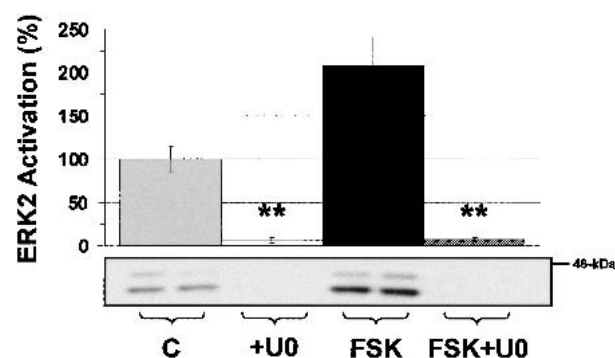


**Figure 3** MEK inhibitors effectively block ERK activation in the mouse hippocampus. Representative Western blots and densitometric analysis of ERK2 (p42 mitogen-activated protein kinase) activation in area CA1 of mouse hippocampal slices treated with vehicle (C; gray bar,  $n = 8$ ), 20  $\mu\text{M}$  U0126 (+U0; white bar,  $n = 9$ ), 50  $\mu\text{M}$  forskolin (FSK; black bar,  $n = 6$ ), or forskolin plus U0126 (FSK+U0; striped bar,  $n = 6$ ).  $**P < 0.001$ .

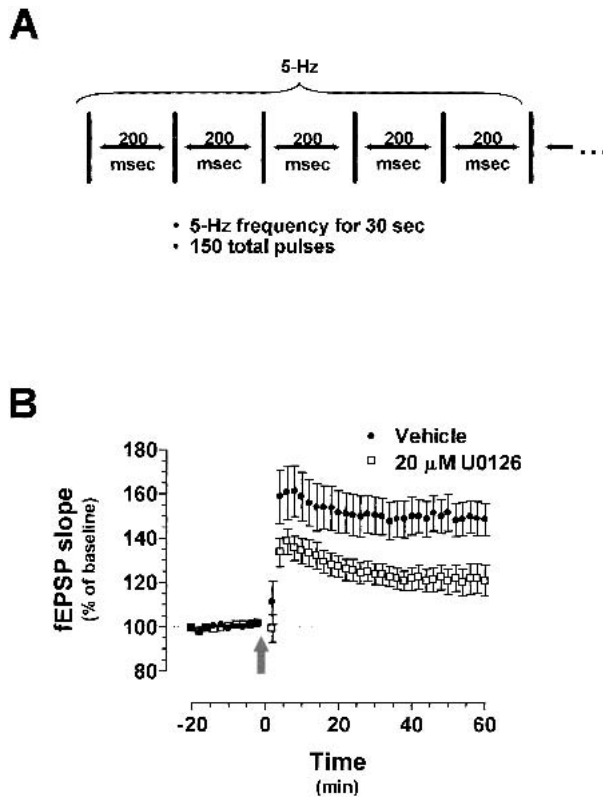


**Figure 4** U0126 impairs long-term potentiation (LTP) induced with  $\theta$  frequency stimulation (TFS) in the mouse hippocampus. (A) Schematic depicting TFS. This LTP induction paradigm consists of 150 single pulses delivered at 5 Hz. (B) LTP induced with TFS (TFS-LTP) is impaired in the presence of the MEK inhibitor ( $n = 11$  slices) compared with vehicle-treated control slices ( $n = 11$  slices). The thick arrow represents the 30 sec of TFS. fEPSP = field Excitatory Postsynaptic Potential

of LTP, dependent on the pattern of stimulation used to evoke LTP. Because the pattern of stimulation was so important in determining the necessity for ERK, we focused on what role (if any) ERK had *during* the LTP-inducing stimulation. Previous investigators have emphasized the importance of action potential firing during  $\theta$  burst and  $\theta$  pattern stimulation in mice (Winder et al. 1999; Watabe et al. 2000; Dudek and Fields 2001); therefore, we investigated the effect of these LTP-induction protocols on neuronal action potential firing and whether ERK activity played any role in this phenomenon.

Evaluating the level of action potential production in the field recordings required a more accurate readout of somatic activity than dendritic or synaptic activity. Therefore, for these experiments, we positioned the recording electrode in stratum pyramidale of area CA1 rather than in stratum radiatum. In order to quantify action potential firing during the TBS, we analyzed field recordings by counting the number of population spikes generated in each burst of four pulses. In setting criteria for what would constitute a

spike, we chose to define a spike as any downward deflection within the EPSP that extended below baseline.

In vehicle-treated control slices, no population spikes meeting this criterion were generated during the first burst of four pulses (Fig. 6A). However, the likelihood of evoking action potentials increased dramatically over the course of the three trains of TBS. By the end of the third train of 10 bursts, roughly three spikes were generated in response to each burst of stimulation (Fig. 6A). These data indicate that TBS produces a progressive increase in the excitability of area CA1 pyramidal neurons, such that the response of these neurons to the same stimulus increases over the course of stimulation.

When hippocampal slices were exposed to 20  $\mu$ M U0126, the production of population spikes during TBS was significantly attenuated. As with control slices, U0126-treated slices displayed few spikes in response to the first

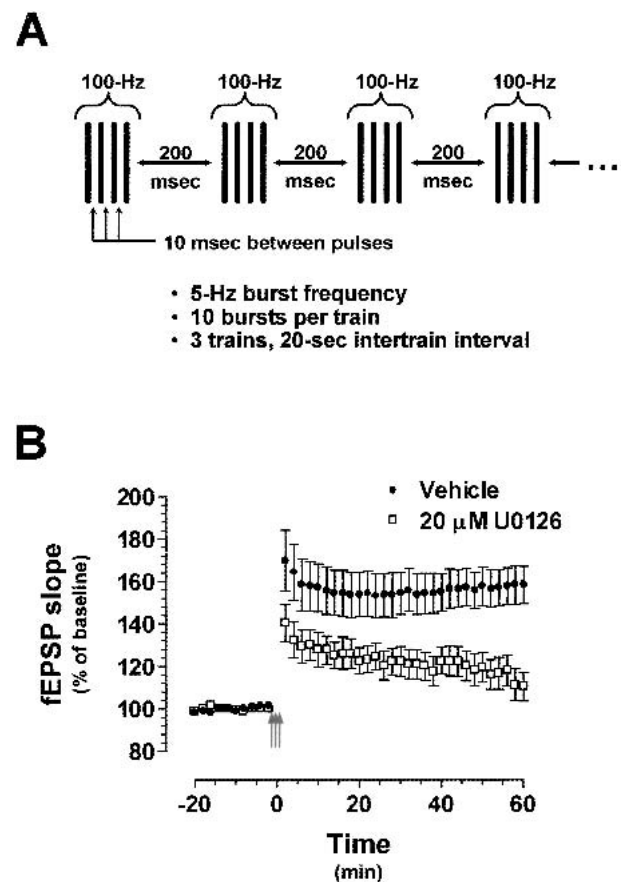


**Figure 5** Long-term potentiation (LTP) initiated by  $\theta$ -burst stimulation (TBS) requires ERK activation in the mouse hippocampus. (A) Schematic depicting TBS. This LTP induction paradigm consists of three trains of 10 high-frequency bursts delivered at 5 Hz. (B) LTP induced with TBS (TBS-LTP) is significantly impaired in the presence of 20  $\mu$ M U0126 ( $n = 13$  slices) compared with vehicle-treated control slices ( $n = 12$  slices). The three red arrows represent the three TBS trains. fEPSP = field Excitatory Postsynaptic Potential

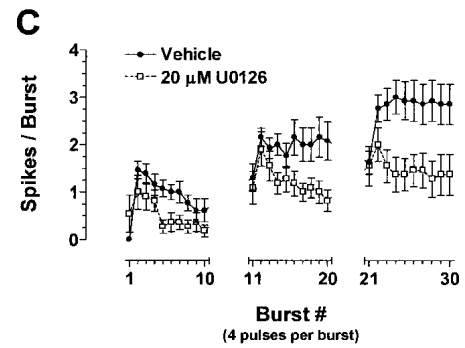
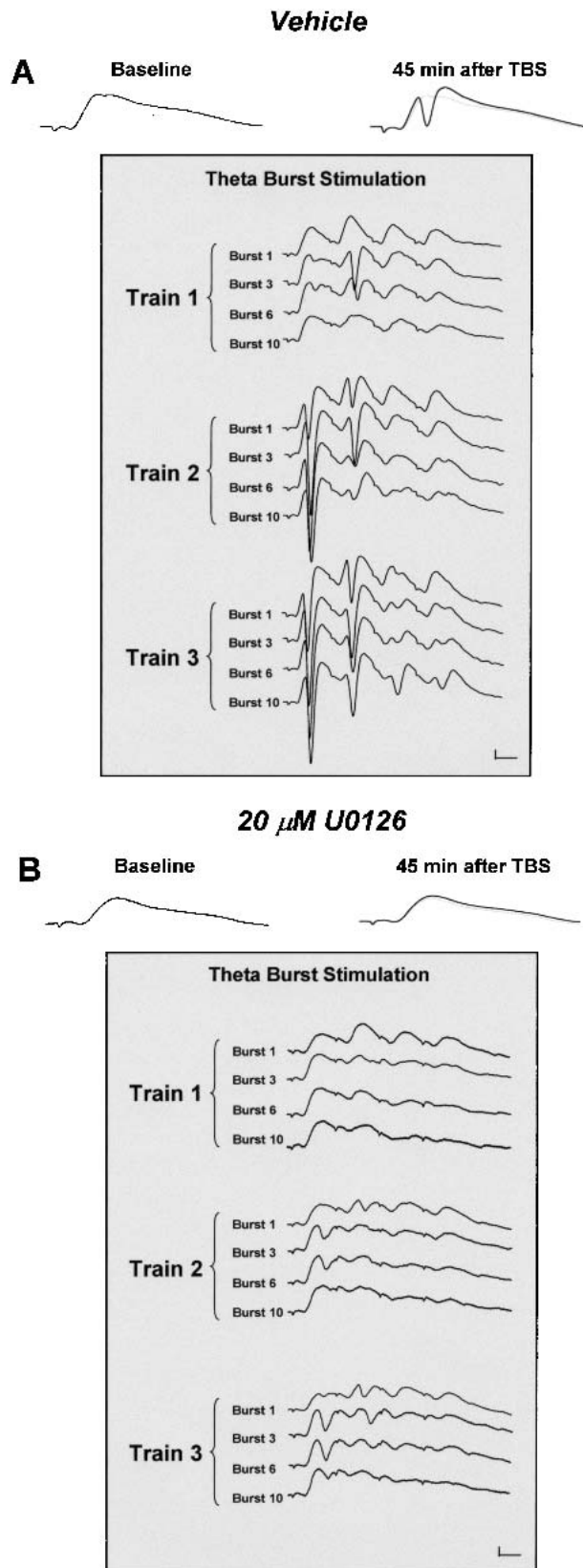


**Figure 6** Increased action potential firing over the course of  $\theta$ -burst stimulation (TBS) is blocked by MEK inhibitors. (A) Representative traces in response to TBS from a vehicle-treated slice. Note the profound difference in spiking between the first and last bursts of the stimulation paradigm. Scale bars (bottom right corner of shaded box) are 1 mV by 5 msec. (B) Representative traces in response to TBS from a slice treated with U0126. Compared with controls, there is much less difference in spiking between the first and last bursts of the stimulation paradigm. Scale bars are 1 mV by 5 msec. (C) Increased spiking during TBS is modulated by ERK. Population spike counts recorded in stratum pyramidale of hippocampal area CA1 during TBS in slices pretreated with vehicle ( $n = 13$  slices) or 20  $\mu$ M U0126 ( $n = 11$  slices). Slices exposed to vehicle showed a progressive increase in spike generation during TBS; administration of U0126 impaired this enhanced spiking.

burst of pulses (Fig. 6B). Over the course of the three trains of bursts, action potential production in these hippocampal slices increased but at a slower rate than in control slices (Fig. 6C). During the third train of bursts, the mean number of population spikes observed in control slices was more than twice the average seen in slices exposed to the MEK inhibitor. These data indicate a role for ERK activation in acute regulation of the likelihood of action potential firing during TBS.

In an additional series of studies, we assessed the NMDA receptor dependence of the increased action potential firing over the course of the TBS. As expected, the NMDA receptor antagonist APV (50  $\mu$ M) blocked LTP induction (data not shown; see also Fig. 2). NMDA blockade also significantly attenuated but did not completely block the increased action potential firing during the period of TBS (Fig. 7). These data indicate that the ERK-dependent temporal integration process operating during TBS could be downstream of the NMDA receptor. In a companion experiment to this series, we attempted to determine if modulation of Gamma Amino Butyric Acid (GABA)-ergic transmission contributed to ERK-dependent increases in action potential firing during TBS (Costa et al. 2002). However, in these studies, blockade of GABA receptors with bicuculline (plus 4 mM magnesium) led to large increases in cellular excitability that precluded assessment of the time-dependent increases in action potential firing over the course of the TBS protocol (see Fig. 7), although there was some detectable activity-dependent increase in action potential firing even in the presence of bicuculline.

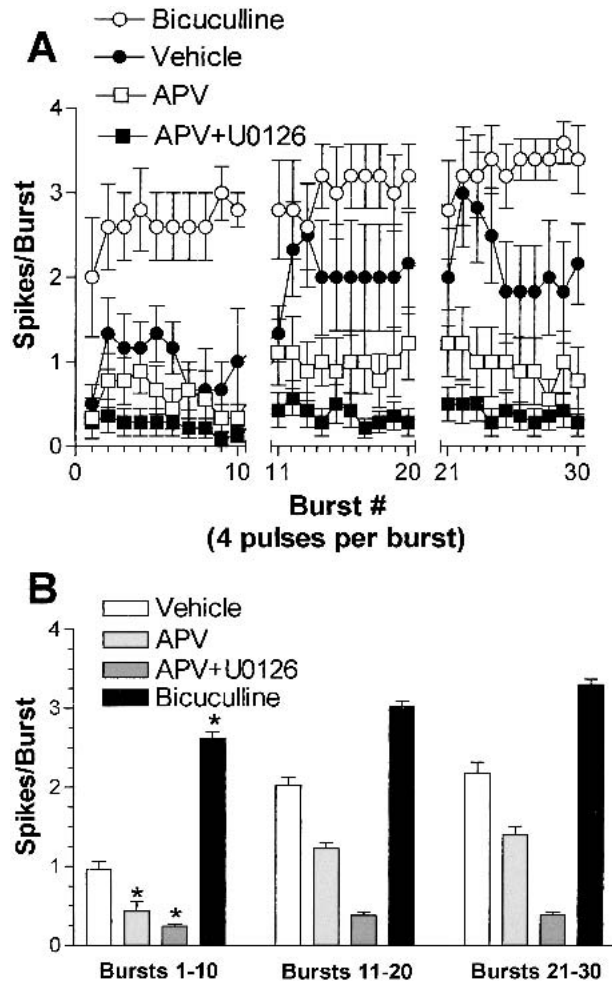


**Figure 7** Effects of APV and bicuculline on increased action potential firing with  $\theta$ -burst stimulation (TBS). (A) Population spike counts recorded in stratum pyramidale of hippocampal area CA1 during TBS in slices pretreated with vehicle ( $n = 6$  slices), 30  $\mu$ M bicuculline ( $n = 6$  slices), 5  $\mu$ M APV ( $n = 7$  slices), or 5  $\mu$ M APV/20  $\mu$ M U0126 ( $n = 14$  slices). All slices showed a progressive increase in spike generation during TBS. (B) Results from panel A showing the average of each set of bursts. Compared with vehicle treated slices for the first set of bursts (bursts 1–10), bicuculline treated slices showed an increase in spike generation. Slices treated with APV showed a significant reduction in spike generation, which was attenuated further with the combination of APV and U0126. (\* $P = 0.0001$ ).

To ascertain if the ERK-dependent temporal integration process is downstream of NMDA receptor activation, we examined whether conjoint application of APV and U0126 would lead to further reductions in activity-dependent increases in action potential firing. In other words, we determined if U0126 could block the residual increase in spiking that occurred in the presence of APV. We found that U0126 further reduced the TBS-associated increase in spiking with APV present (Fig. 7). These data indicate that there are additional NMDA receptor-independent, ERK-dependent

processes operating as a temporal integration mechanism with TBS induction of LTP.

In our next series of experiments, we assessed population spikes during the TFS protocol. For these experiments, we used a dual-recording electrode technique. The stimulating electrode remained in hippocampal area CA3 and activated Schaffer collateral fibers innervating area CA1. One recording electrode was positioned in stratum radiatum of area CA1, whereas another electrode was placed in stratum pyramidale. For each stimulus, the initial slope of the EPSP recorded in stratum radiatum and the amplitude of the population spike recorded in stratum pyramidale were measured during the 5-Hz, 30-sec TFS paradigm.

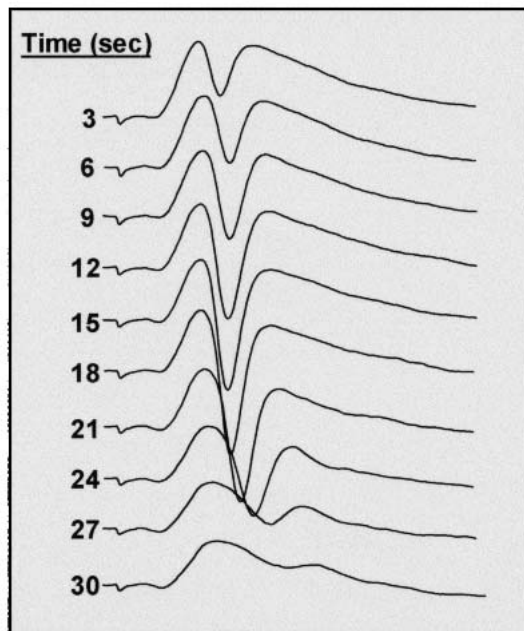
TFS (5 Hz, 30 sec) also resulted in a short-lived change in population spikes during the 30 sec of 5-Hz stimulation. In Figure 8A, recordings are shown from stratum pyramidale of hippocampal area CA1. The five responses within each second of stimulation were binned and averaged, resulting in 30 EPSP traces (Fig. 8A). For each averaged trace, the EPSP slope and population spike amplitude were measured. For roughly the first 20 sec of the stimulation, the amplitude of the population spike increased dramatically. Meanwhile, over this same time period, the EPSP slope recorded in stratum radiatum gradually declined. Therefore, the ratio of the population spike amplitude to the EPSP slope increased over time, indicating EPSP-to-spike potentiation (E-S potentiation; Fig. 8C).

Spike-EPSP ratios were also monitored in slices exposed to the MEK inhibitor U0126. In these slices, the amplitude of population spikes during TFS increased significantly, peaking at  $\sim 20$  sec (Fig. 8B). As in vehicle-treated slices, EPSP initial slopes also diminished over time in response to TFS. Therefore, the spike:EPSP ratio increased in these slices, showing no overall difference between vehicle- and U0126-treated slices (Fig. 8C), although there was a distinct trend toward U0126 diminishing the increase in spike firing at early time points in TFS. These data indicate that, although ERK is necessary for TFS-LTP, it may not be critical in altering neuronal excitability as appears to be true in the  $\theta$ -burst protocol. However, we certainly cannot eliminate the possibility that the early attenuation we observed with MEK inhibition contributes to the effect of U0126 in blocking TFS-LTP.

### Characterization of ERK1 Null Mice

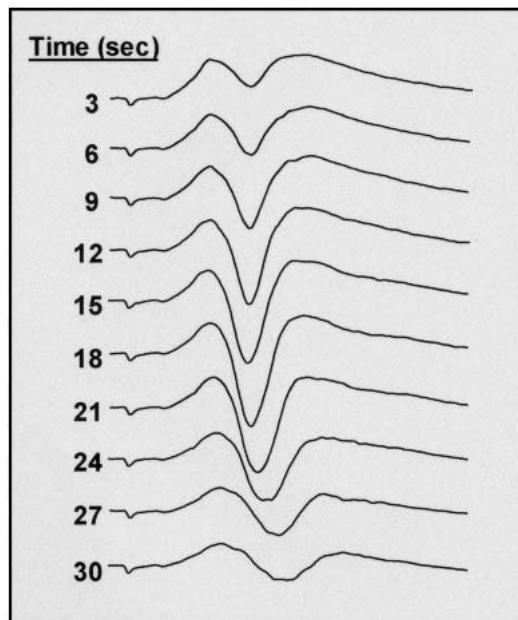
Results from the previous section help establish the ERK isoforms of MAPK as critical players in certain forms of hippocampal plasticity (e.g., mouse TBS-LTP). However, the relative contributions of the two ERK isoforms to hippocampal synaptic plasticity have not been addressed. In the mouse hippocampus, as in the rat hippocampus, stimulation of the cAMP cascade leads to activation of both ERK1 and ERK2 (see Fig. 3). However, on the basis of the relative levels of phospho-ERK detected in these assays, ERK2 ap-

### A Vehicle Theta Frequency Stimulation



### B 20 $\mu$ M U0126

#### Theta Frequency Stimulation



appears to be the predominant isoform phosphorylated following cAMP-dependent Protein Kinase stimulation or in the basal condition. If ERK2 is indeed preferentially acti-

### C Dual Recording

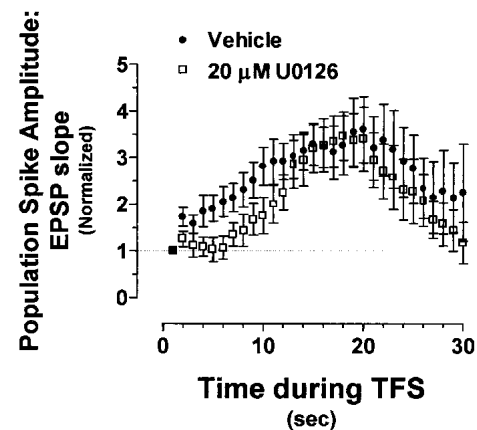
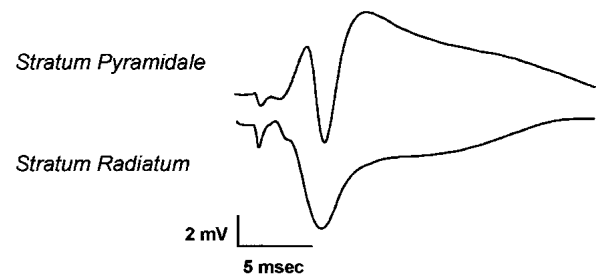


**Figure 8** Increased population spike amplitude over the course of  $\theta$  frequency stimulation (TFS). (A) Representative traces in response to TFS (5 Hz, 30 sec) from a vehicle-treated slice. During TFS, the amplitude of the population spike grows, whereas the slope of the EPSP gradually decreases. (B) Representative traces in response to TFS (5 Hz, 30 sec) from a U0126-treated slice. Although U0126 impairs TFS-long-term potentiation (LTP), the drug appears to have little effect on the enhancement of the population spike during the stimulation paradigm. (C) Transient E-S potentiation during TFS in the mouse hippocampus. The ratio of the population spike (measured in stratum pyramidale) to the EPSP slope (measured in stratum radiatum) was investigated during TFS. Over the course of the 30 sec of stimulation, the pSpike:EPSP ratio was enhanced. This alteration in E-S coupling was characterized by a gradual decline in the EPSP slope in conjunction with increasing population spike amplitude during TFS. The data was normalized to the initial S-E ratio measured 1 sec into the LTP-inducing stimulation.

vated in the hippocampus, what role is the *ERK1* isoform of MAPK playing in synaptic plasticity? The availability of ERK1 knockout mice provided a powerful tool with which to assess the specific function of this isoform at the level of the synapse. Therefore, we performed physiological characterization of the hippocampus from these mutant mice with an emphasis on probing the role of ERK1 in TBS-induced LTP at the CA3-CA1 synapse.

We have previously reported that loss of the ERK1 isoform of MAPK had no deleterious effect on baseline synaptic transmission, paired-pulse facilitation, and HFS-induced LTP at Schaffer collateral synapses (Selcher et al. 2001). These results indicate that ERK1 is not necessary for

normal hippocampal synaptic transmission and is not an integral component of the machinery underlying short-term plasticity. Similarly, in these previous experiments, HFS-LTP induced with two 1-sec, 100-Hz tetani separated by 20 sec was not different between *ERK1* knockout mice and littermate controls in either post-tetanic potentiation or HFS-LTP (Selcher et al. 2001). Because the MEK inhibitor study described earlier indicates that overall ERK activation is not necessary for HFS-LTP in the mouse hippocampus, in retrospect, this is not a particularly surprising result.

In the present studies, MEK inhibition did, however, impair LTP induced with the two  $\theta$  protocols we used earlier. Therefore, we tested whether ablation of the *ERK1* gene had any effect on an ERK-dependent form of LTP. Bursts of HFS delivered at the  $\theta$  frequency (TBS) produced stable LTP in hippocampal slices taken from littermate control mice (Fig. 9A; 45 min after TBS:  $135.3 \pm 7.2\%$  of baseline). *ERK1* null mice exhibited LTP indistinguishable from that of controls in response to the TBS paradigm (45 min after TBS:  $138.3 \pm 10.2\%$  of baseline for *ERK1* knockout slices;  $P > 0.05$ ). Based on our previous characterization of these mice, the lack of an LTP phenotype would not appear to be due to any compensatory change in ERK2 protein levels or enhanced ERK2 activation in the *ERK1* knockout mice (Selcher et al. 2001). To directly test the possibility of compensation in the *ERK1* knockout mice, we assessed the effect of pharmacological inhibition of MEK on  $\theta$  burst LTP in these *ERK1*-deficient mice. Application of 20  $\mu$ M U0126 produced a similar attenuation of TBS-LTP in the *ERK1* knockout and wild-type slices (45 min after TBS:  $117.9 \pm 4.9\%$  of baseline for *ERK1* knockout slices treated with U0126;  $P < 0.01$ ; data not shown). These data indicate a specific role for ERK2 activation in TBS-LTP. However, one caveat is that, compared with the amount of LTP obtained in C57BL/6 controls during the inhibitor studies, the average LTP elicited in wild-type 129/SvImJ control slices was noticeably lower, indicating that the 129/Sv background strain is not a particularly good choice for plasticity studies. Despite this technical caveat, these data generally support the hypothesis that area CA1 hippocampal LTP is not dependent on the activity of the ERK1 isoform of MAPK.

In an additional series of experiments, we found that with  $\theta$  frequency (5 Hz, 30 sec) stimulation, only very modest potentiation was induced in wild-type slices (45 min after TFS:  $117.9 \pm 6.0\%$  of baseline, data not shown). Hippocampal slices taken from *ERK1* knockout mice also exhibited a meager amount of LTP in response to TFS and there was no statistical difference between the two sets of mice (45 min after TFS:  $106.2 \pm 3.0\%$  of baseline;  $P > 0.05$ ). However, because of the lack of robust LTP in control slices, an impairment would have been difficult to detect and thus the existence of a deficit in this form of LTP remains a possibility. This was not the first demonstration of

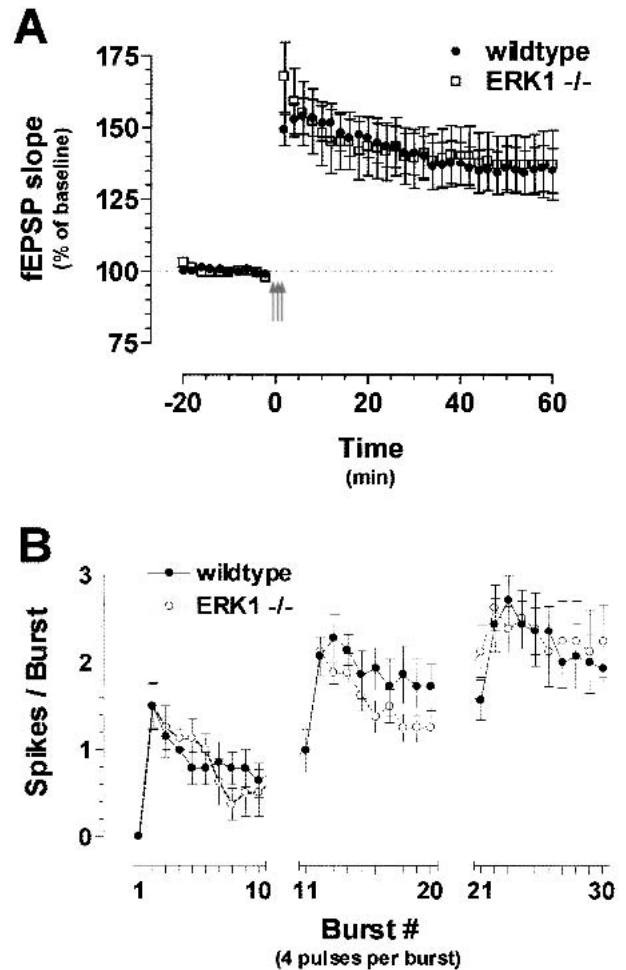


**Figure 9** Long-term potentiation (LTP) is unimpaired in *ERK1* knockout mice. High-frequency stimulation-LTP is unimpaired in *ERK1* knockout mice. (A) Mice lacking the ERK1 isoform display normal  $\theta$ -burst stimulation (TBS)-LTP.  $\theta$ -burst stimulation consists of three trains of 10 high-frequency bursts delivered at 5 Hz. LTP induced with TBS (TBS-LTP) was normal in *ERK1* knockout mice ( $n = 10$  slices) compared with wild-type controls ( $n = 14$  slices). The three arrows represent the three TBS trains. fEPSP = field Excitatory Postsynaptic Potential. (B) *ERK1* null mice exhibit normal postsynaptic spiking during TBS. Population spike counts recorded in stratum pyramidale of hippocampal area CA1 during TBS in slices taken from *ERK1*-deficient mice ( $n = 8$  slices) or wild-type controls ( $n = 14$  slices). Both sets of slices showed significant increases in action potential firing, and there was no difference in spike counts between the two strains.

reduced  $\theta$  LTP in mice on a 129/Sv background (Nguyen et al. 2000), but this possible strain effect does confound interpretation of the results of these experiments.

Although the results we described earlier indicate that the ERK1 isoform of MAPK does not play a predominant role in synaptic plasticity, those particular experiments focused entirely on the synaptic aspect of LTP, increases in EPSP slope. The experiments in the previous section indicate that ERK plays a role in the regulation of neuronal



excitability; therefore, we performed an additional experiment to determine if loss of the ERK1 isoform of MAPK was involved in acute alterations in population spike production with  $\theta$ -burst LTP induction protocols. For this experiment, we again recorded from stratum pyramidale and counted the number of population spikes generated during TBS-LTP. Similar to the results described earlier, stimulation during the first burst of pulses did not lead to action potential generation in control slices taken from wild-type littermates (Fig. 9B). The likelihood of firing an action potential increased rather quickly during TBS-LTP. These data confirm the finding in the previous section indicating that TBS produces a progressive increase in the excitability of the postsynaptic hippocampal neurons.

Unlike the pharmacologic manipulation of the ERK MAPK cascade, the specific genetic targeting of the *ERK1* isoform in the knockout mice had no effect on spike generation. In a manner almost identical to controls, hippocampal slices from *ERK1* knockout mice exhibited a progressive increase in the likelihood of firing an action potential during TBS (Fig. 9B). By the end of the third train of stimulation, each burst generated roughly 2.5 spikes per burst. There was no significant difference between the spiking observed in *ERK1* null mice compared with wild-type controls. These data indicate that, although ERK appears to be a critical modulator of the enhanced spiking in general (see Fig. 6 for comparison), the presence of the ERK1 isoform of MAPK is not critical to this function; in other words, ERK1 does not appear to play a predominant role in regulating action potential generation during TBS.

## DISCUSSION

Considerable evidence already exists implicating ERK in various forms of synaptic plasticity in a wide variety of systems. Long-term facilitation of the sensory-motor neuron synapse in *Aplysia* causes translocation of ERK into the nucleus of presynaptic neurons. Furthermore, inhibition of ERK by either anti-MAPK antibodies or MEK inhibition blocks long-term, and short-term, facilitation of the sensory-motor synapse (Martin et al. 1997; Michael et al. 1998; Chin et al. 2002). ERK has also been shown to be activated during an in vitro Pavlovian conditioning paradigm in *Hermisenda*, and this activation is blocked by pretreatment with PD098059 (Crow et al. 1998). In addition to the present study, activation of the ERK isoforms of MAPK have been demonstrated to be necessary for the induction of NMDA receptor-dependent LTP in area CA1 of the hippocampus (English and Sweatt 1996, 1997; Atkins et al. 1998; Impey et al. 1998; Winder et al. 1999; Wu et al. 1999; but also see Liu et al. 1999), NMDA receptor-independent LTP in area CA1 (Kanterewicz et al. 2000), LTP in the dentate gyrus (Coogan et al. 1999), LTP in vivo (Davis et al. 2000; Rosenblum et al. 2000), and LTP of the amygdalar inputs into the insular cortex (Jones et al. 1999). In addition, long-term depression

in the rat hippocampus is associated with long-lasting decreases in ERK immunoreactivity (Norman et al. 2000).

Given the requirement for ERK in a wide variety of forms of hippocampal synaptic plasticity and in relevant learning tasks at the behavioral level, we focused on improving our understanding of the mechanisms by which ERK contributes to the induction of lasting changes in synaptic strength. To this end, we inhibited ERK activation in the mouse hippocampus and tested the effect of this pharmacological manipulation on the induction of long-term potentiation.

Surprisingly, inhibiting ERK activation appears to produce differential effects, depending on the species, on hippocampal long-term potentiation induced with an HFS protocol consisting of two trains of 1-sec, 100-Hz tetani. In vehicle-treated hippocampal slices from rats, HFS results in a significant and stable increase in the initial slope of the EPSP. In a number of previous studies, this enhancement in synaptic strength was found to be blocked by application of any of three MEK inhibitors: SL327, PD098059, or U0126 (English and Sweatt 1997; Atkins et al. 1998; Wu et al. 1999). In the present studies on the mouse hippocampus, however, MEK inhibitors had no effect on LTP induced with this high-frequency tetanic stimulation. These findings indicate that LTP induced with a pair of 100-Hz tetani requires ERK activation in rats but not in mice. This would then indicate the novel idea that these two closely related species do not use identical molecular mechanisms for the induction of this particular form of synaptic plasticity.

In a separate set of experiments, the ability of the MEK inhibitor U0126 to block cAMP-stimulated ERK activation in mice was also tested. Previously, Roberson et al. (1999) demonstrated that MEK inhibitors were effective at attenuating forskolin-induced increases in ERK activation in area CA1 of the rat hippocampus. As in the rat, 20  $\mu$ M U0126 completely blocked stimulated phospho-ERK levels following treatment with 50  $\mu$ M forskolin in area CA1 of hippocampal slices prepared from C57BL/6J mice. Thus, it appears that the disparate LTP results do not stem from differential efficacy of the MEK inhibitors in the two systems.

The behavioral relevance of traditional HFS paradigms such as the one described earlier (two trains of 1-sec, 100-Hz tetanic stimulation) has been questioned in light of the fact that this amount of activity would rarely, if ever, occur in a normal brain. However, LTP in the hippocampus can also be induced with naturalistic patterns of stimulation that emulate the firing pattern of hippocampal pyramidal neurons. This natural brain rhythm, called the  $\theta$  rhythm, occurs as a rhythmic oscillation in hippocampal activity in the 4-12-Hz range during exploratory locomotor behaviors (Bland et al. 1984): Short bursts of 100-Hz stimulation delivered at 200 msec intervals (to fall within the 4-12 Hz  $\theta$  range) effectively induce LTP lasting weeks in vivo (Larson et al. 1986; Staubli and Lynch 1987).

We tested the effect of MEK inhibition on two LTP induction protocols that mimicked the endogenous  $\theta$  rhythm. Unlike the results obtained with LTP induced by high-frequency tetani, LTP induced by patterned stimulation in the  $\theta$  frequency required ERK activation. U0126-treated slices showed impaired (but not completely blocked) LTP elicited by “TFS” consisting of stimulation at 5 Hz for 30 sec. These data are consistent with results obtained by Winder et al. (1999) and Watabe et al. (2000), who have also demonstrated a regulatory role for ERK in this form of LTP. ERK was also found to be necessary for LTP induced with a TBS protocol (high-frequency bursts at 5 Hz), in good agreement with these findings.

Taken together, these findings build a convincing argument for a requirement of the ERK isoforms of MAPK in the molecular events that underlie information storage at both the synaptic and behavioral levels. Another goal of the present study was to address the specific contribution of one of these ERK isoforms. To this end, *ERK1* knockout mice were tested using TBS protocols.

One important caveat to this study, as with other studies involving knockout animals, involves developmental effects of the mutation. The fact that the gene and its product were missing throughout development means that the knockout affects every ERK1-dependent function during development. Because the ERK MAPK pathway is so important developmentally, the potential for these types of effects was especially worrisome. In a previous study, we analyzed whether the absence of ERK1 during development allowed compensatory mechanisms to emerge that could potentially mask the normal role of ERK1. In our previous study, we found that *ERK1* null mice, however, appeared to show normal anatomical and functional development (Selcher et al. 2001). Similarly, no obvious compensatory changes were seen in the basal levels of ERK2 or in stimulated levels of phosphorylated ERK2 in the hippocampi of knockout mice.

Mice deficient in ERK1 also showed no impairments in tests of hippocampal physiology. The present studies, combined with our prior results (Selcher et al. 1999), show that ERK1 knockout mice display normal synaptic transmission, short-term plasticity, and long-term plasticity, as tested with three different LTP induction paradigms. Both HFS and TBS paradigms produced significant LTP in ERK null mice that was indistinguishable from controls. A recent study examining a different ERK1 knockout mouse was, for the most part, consistent with our hippocampal slice physiology results (Mazzucchelli et al. 2002). As in our studies, this group found no impairment in LTP induced with tetanic stimulation in ERK1 mutant mice. Although TBS produced significantly less LTP in their *ERK1* null mice compared with C57BL/6 wild-type controls, the effect was quite modest and not qualitatively different than the results we report here. Interestingly, the *ERK1* knockout mice examined in the Mazzucchelli study did exhibit a robust increase in LTP

at neocortical inputs to the nucleus accumbens, indicating that ERK1 may play a more essential role in synaptic plasticity in the striatum.

Thus, these studies, coupled with a number of recent findings, indicate that ERK2 may be more selectively involved in mammalian learning. Relative to ERK1, for example, the ERK2 isoform of MAPK shows higher basal levels of activation in the hippocampus, as assessed using phospho-selective antibodies (demonstrated in Fig. 3 of the present paper). Hippocampal ERK2 also displays a high degree of responsiveness to a variety of signal transduction pathways critical to synaptic plasticity and learning (Roberson et al. 1999; Schmid et al. 1999; Norman et al. 2000). More interestingly, perhaps, selective activation of ERK2 has been previously demonstrated following induction of a physiological model for learning. In these experiments, phospho-ERK2 but not phospho-ERK1 levels were significantly increased in area CA1 of the rat hippocampus 1 h after delivery of LTP-inducing tetanic stimulation (English and Sweatt 1996). The preferential activation of the ERK2 isoform of MAPK in the same region of the rat hippocampus was also observed in experimental animals 1 h after exposure to contextual fear conditioning (Atkins et al. 1998).

### A Role for ERK in Regulating Activity-Dependent Increased Action Potential Firing

To investigate ERK-dependent mechanisms operating during LTP-inducing stimulation protocols, we monitored spike production in the cell body layer of the hippocampus during the period of  $\theta$ -like stimulation. In field recordings, population spikes signify synchronous firing of action potentials in the postsynaptic CA1 pyramidal neurons. Baseline, low-frequency stimulation at test stimulus intensity rarely resulted in the generation of prominent population spikes. However, TBS produced a significant amount of postsynaptic spiking. On further analysis, we found that the likelihood of spike production increases progressively over the course of the three trains of TBS in this LTP induction protocol. This increase in the response of the postsynaptic cell indicates that  $\theta$  stimulation results in a significant acute increase in CA1 pyramidal cell excitability, although other possibilities such as altered GABAergic modulation should also be considered.

Is this increase in spike firing really due to a change in excitability? One alternative possibility would be that synaptic facilitation was the true cause of the increased postsynaptic response. If the amplitudes of the individual EPSPs were enhanced during TBS, the additive effect of larger depolarizations on the soma might be sufficient to trigger action potentials independent of a change in postsynaptic excitability. Because enhanced EPSPs are documented following this stimulation (see Fig. 6, for example), this alternative to increased excitability is certainly conceivable. In-

deed, paired-pulse facilitation data from the mouse hippocampus demonstrates an ~30% increase in the initial slope of the second of two EPSPs when two pulses are delivered with an interstimulus interval of 200 msec. However, this reveals little about what happens during repeated trains of stimulation. Inspection of the traces recorded in the cell body layer during stimulation reveals no increase in the amplitude or slope of the field EPSPs within a train. In fact, the field recordings indicate that the field EPSPs diminish over the course of each 10-burst train; in other words, the slices exhibit synaptic depression rather than synaptic facilitation. This finding indicates that the enhanced response to the bursts of stimulation cannot be attributed to an increase in synaptic input and likely represents an increase in excitability.

Inhibition of ERK activation dampened TBS-induced increases in excitability. By the end of the TBS, action potential firing in U0126-treated hippocampal slices was attenuated to half the level observed in vehicle-treated control slices. These data indicate that, for specific patterns of physiologic stimulation, ERK may function in the regulation of neuronal excitability in hippocampal area CA1. This interpretation is in good agreement with prior studies by Winder et al. (1999) and Watabe et al. (2000), who reached a similar conclusion based on studies of TFS in area CA1.

Interestingly, U0126-treated slices were unimpaired in their response to the first burst of all three 10-burst trains (see Fig. 6). One explanation for this observation would be the existence of two different mechanisms underlying the increased excitability produced by TBS. If this speculation is true, the data indicate that one mechanism might explain the increase in excitability over the course of each train. This ERK-dependent enhancement occurs over a 2-sec time period (10 bursts delivered at 5 Hz) and appears to decay during the 20-sec delay between TBS trains. The other mechanism would seemingly be independent of ERK and would be responsible for the overall rise in excitability seen from one TBS train to the next (in Fig. 6C, compare bursts #1, 11, and 21).

Uncertainty remains regarding what role the additional action potential firing plays in LTP. The necessity for postsynaptic spiking in LTP induced with “ $\theta$ -like” stimulation protocols has been previously addressed (Thomas et al. 1998). Thomas and colleagues demonstrated that  $\theta$  frequency (5 Hz) stimulation induced both complex spike bursting, a characteristic mode of hippocampal action potential firing in vivo, and LTP. This LTP could be blocked by pharmacologic manipulations that specifically eliminated the complex burst spiking without affecting single action potential generation. This result indicates a requirement for postsynaptic spiking in LTP induced with TFS.

Using a stimulation protocol similar to the one used in Thomas et al. (1998), we examined postsynaptic excitability during TFS of CA3 afferents onto CA1 pyramidal cells.

Instead of counting spikes, as was done with the TBS protocol, the EPSP slopes and population spike amplitudes from traces acquired during TFS stimulation were analyzed. The ratio between these two measures changed dramatically over the course of the 30 sec of 5-Hz stimulation, indicating an increase in the spike-to-EPSP ratio during the first 20 sec of stimulation. This increase in excitability disappeared during the final 10 sec of stimulation, as synaptic depression severely dampened postsynaptic responses. Although ERK activation was necessary for LTP induced with TFS, application of U0126 had no significant effect on either the increases in population spike amplitude or the corresponding increase in EPSP-spike coupling, indicating that ERK may be playing a different role in this form of LTP than it is in the TBS-LTP paradigm. However, we should note that there is an effect of MEK inhibition on spike generation early in TFS (see times 0–12 sec in Fig. 8C), which should not be discounted as potentially contributing to the block of TFS-LTP.

The progressive increase in spiking observed during TBS represents a prime illustration of temporal integration. Delivery of the first stimulus pulse in the TBS induction tetani did not produce a sufficient effect postsynaptically to fire an action potential. However, the biochemical processes activated by this stimulus do not terminate instantaneously, but rather decay over time. The initial stimulus pulse may serve to amplify subsequent stimuli, thereby enhancing the effect of each successive stimulus pulse. Thus, temporal integration may serve as a mechanism by which multiple, spaced tetanic stimuli (e.g., TBS) can produce unique effects, such as increased postsynaptic spike generation. The fact that MEK inhibitors attenuate this increased spiking strongly indicates that ERK is functioning as a component of a temporal integrator in response to TBS.

If ERK is functioning as a temporal integrator, how exactly does it amplify the effects of subsequent stimuli? More specifically for TBS, what effector is ERK acting on to enable the increased spike generation? Potassium ( $K^+$ ) channels serve as the principal regulators of membrane excitability in the central nervous system, and potassium channels can also regulate membrane excitability via their influence over the size and shape of action potentials as they back-propagate into the dendrites. The decreasing amplitude of action potentials as they back-propagate into the dendrites results from an increasing density of transient A-type  $K^+$  channels with distance from the soma (Hoffman et al. 1997). We hypothesize that modulation of A-type channels, specifically the Kv4.2 isoform, contribute to the ERK-mediated acute alteration in pyramidal neuron excitability, as these channels are known to be substrates for ERK (Adams et al. 2000). Recent evidence from Johnston and colleagues supports this idea by demonstrating that MEK inhibitor application leads to down-regulation of A-type  $K^+$  currents in CA1 pyramidal neurons and reduces the boost-

ing of dendritic action potentials by EPSPs (Watanabe et al. 2002; Yuan et al. 2002). Other potential mechanisms that could subserve the increased spike production during  $\theta$  stimulation include modulation of sodium ( $\text{Na}^+$ ) channels, which regulate the currents responsible for the depolarizing spikes of the action potential, and modification of inhibitory circuits subserved by GABAergic interneurons. To date, however, no evidence exists of ERK regulation of  $\text{Na}^+$  channels or inhibitory GABAergic connections. It is important to bear in mind that these actions on excitability likely reside upstream of the NMDA receptor (see Fig. 7) and may serve as a firing-pattern dependent gating mechanism that contributes to the induction of LTP.

## MATERIALS AND METHODS

Animals were housed on a 12 h-light/dark schedule. All experiments were performed in accordance with the Baylor College of Medicine Institutional Animal Care and Use Committee and with national regulations and policies.

ERK1 knockout and littermate wild-type mice were generated on a mixed 129S1/SvImJ  $\times$  CD1 genetic background. The genetic background of the subjects used in these experiments was 98% 129/SvImJ following multiple (roughly six or seven) backcrossings. ERK1 null mice and littermate wild-types were shipped from Case Western Reserve School of Medicine and were held at Baylor College of Medicine in quarantine for ~4 weeks. Behavioral testing was begun 1 week following release from quarantine.

129S1/SvImJ mice, ERK1 null mice, and their littermate controls were used in physiology experiments after they were in the behavior studies. In addition, C57BL/6J mice (Baylor barrier) were also used. Unless otherwise stated, C57BL/6J mice, 4–8 weeks of age, were used for all hippocampal slice physiology studies.

### Drugs

U0126 was dissolved in DMSO and diluted into saline solution (artificial cerebrospinal fluid [ACSF]; see following) to give the desired final concentration (with a final DMSO concentration of 0.1%). APV (DL-AP5; Tocris) was dissolved in 100 mM NaOH and applied at a concentration of 50  $\mu\text{M}$ . U0126 was a generous gift from James Trzaskos and DuPont Pharmaceuticals. In later experiments, U0126 was obtained through Promega.

### Preparation of Hippocampal Slices

Hippocampal slice preparation and electrophysiology were performed as described (English and Sweatt 1996). Hippocampi of wild-type or mutant mice were rapidly removed and briefly chilled in ice-cold cutting saline (containing 110 mM sucrose, 60 mM NaCl, 3 mM KCl, 1.25 mM  $\text{NaH}_2\text{PO}_4$ , 28 mM  $\text{NaHCO}_3$ , 500  $\mu\text{M}$   $\text{CaCl}_2$ , 5 mM D-glucose, 7 mM  $\text{MgCl}_2$ , and 600  $\mu\text{M}$  ascorbate, saturated with 95%  $\text{O}_2$  and 5%  $\text{CO}_2$ ). Transverse slices 400- $\mu\text{m}$  thick were prepared with a Vibratome and maintained at least 45 min in a holding chamber containing 50% ACSF (containing 125 mM NaCl, 2.5 mM KCl, 1.24 mM  $\text{NaH}_2\text{PO}_4$ , 25 mM  $\text{NaHCO}_3$ , 10 mM D-glucose, 2 mM  $\text{CaCl}_2$ , and 1 mM  $\text{MgCl}_2$ , saturated with 95%  $\text{O}_2$  and 5%  $\text{CO}_2$ ) and 50% cutting saline. The slices were then transferred to a recording chamber and perfused (1 mL/min) with 100% ACSF. Slices were allowed to equilibrate for 60–90 min in a Fine Science Tools interface chamber at 30°C.

## Electrophysiological Characterization

### Set-up and Electrode Placement

For extracellular field recordings, glass recording electrodes were pulled from capillary glass using a horizontal electrode puller (Narishige) and filled with ACSF. Input resistance was tested in these electrodes by applying a current pulse, and the tips were broken off until a resistance of 1–3 M $\Omega$  was obtained ( $R = V/I$ ). Recording electrodes were placed in hippocampal area CA1 in stratum radiatum, stratum pyramidale, or both. Test stimuli were delivered to the Schaffer collateral/commissural pathway with a bipolar Teflon-coated platinum stimulating electrode positioned in stratum radiatum of area CA3. Responses were recorded through a PC using AxoClamp pClamp8 data acquisition software. The maximal slope and peak amplitude of single population EPSPs (downward-deflecting for stratum radiatum recordings and upward-deflecting for stratum pyramidale recordings) were measured online using the data acquisition software. EPSP slope measurements were taken as early as possible after the fiber volley to eliminate contamination by population spikes. For pharmacological studies, U0126 or vehicle were applied for at least 1 h prior to testing and were maintained throughout the recording period.

### Input/Output (I/O) Curves

Test stimuli were delivered and responses recorded at 0.05 Hz; every six consecutive responses over a 2-min period were pooled and averaged. Field excitatory postsynaptic potentials were recorded in response to increasing intensities of stimulation (from 2.5  $\mu\text{A}$  to 45.0  $\mu\text{A}$ ). For the remainder of the physiological protocol, the test stimulus intensity was set to elicit an EPSP that was ~35%–50% of the maximum response recorded during the I/O measurements.

### Paired-Pulse Facilitation

Following I/O curve generation, paired-pulse facilitation, a form of short-term synaptic plasticity, was tested. Two stimulus pulses were applied with varying interpulse intervals ranging from 20–300 msec.

### LTP

LTP was induced after at least 20 min of stable baseline recording. Three different stimulation protocols (with stimulation at test stimulus intensity) were used in these experiments:

HFS consisted of two trains of 1-sec, 100-Hz stimulation with an intertrain interval of 20 sec = 200 pulses total.

TFS consisted of 30 sec of stimulation delivered at 5 Hz (200 msec between pulses) = 150 total pulses.

TBS consisted of three trains of stimuli delivered at 20-sec intervals, each train composed of 10 stimulus bursts delivered at 5 Hz, with each burst consisting of four pulses at 100 Hz (Larson et al. 1986) = 120 total pulses.

### Biochemistry Studies

For in vitro biochemistry studies, hippocampal slices were prepared as described earlier for electrophysiological analysis. Slices were first incubated in 50% cutting saline/50% ACSF, followed by incubation in ACSF at room temperature for 1 h; they were then transferred to a static submersion chamber containing 15 mL of ACSF at 32°C. In other experiments, hippocampal slices underwent pharmacological manipulation within the electrophysiology recording chamber. At the desired time point after pharmacological stimulation of hippocampal slices, the nylon screen supporting the slices was removed from the chamber and placed in a glass Petri

dish on crushed dry ice for rapid freezing. In experiments in which drugs were applied in static submersion chambers, slices were quickly transferred to nylon screens before freezing. Area CA1 was dissected with a scalpel blade under a dissecting microscope. These CA1 subregions were then stored at  $-80^{\circ}\text{C}$  until they were assayed biochemically.

### Western Blotting

Immobilon filters were blocked overnight at  $4^{\circ}\text{C}$  in blocked in BSA-containing Tween/Tris-Buffered Saline (B-TTBS) (in mM: 50 mM Tris-HCl at pH 7.5, 150 mM NaCl, 20  $\mu\text{M}$  sodium orthovanadate, 0.05% Tween-20, 3% bovine serum albumin, 0.01% thimerosal), unless otherwise indicated. All antibody applications were done in B-TTBS, unless otherwise indicated. For each of the Western blots described as follows, control blots in which the primary antibody was excluded demonstrated that all ERK immunoreactivities were due to the primary antibody, and were not a result of nonspecific staining of the detection system (data not shown). All blots were probed with primary antibody followed by incubation with secondary antibody, after which they were developed using enhanced chemiluminescence (Amersham). Blots were washed extensively in TTBS after incubations with secondary antibody and second antibody, or Avidin/Biotin Complex (ABC) reagents (typically four washes, each 12 min).

### Antibodies

#### $\alpha$ -Phospho-ERK

We used two different antisera that selectively recognize phosphorylated ERK MAPKs: an antiphosphotyrosine ERK antiserum (New England Biolabs; raised against a phosphopeptide corresponding to amino acids 196–209 of human ERK1, phosphorylated at tyrosine 204) and an anti-dual-phospho-ERK antiserum (New England Biolabs; selectively detects ERK MAPKs phosphorylated at both threonine 202 and tyrosine 204). Both were used at a dilution of 1:1000. Horseradish Peroxidase (HRP) conjugated secondary antibody was used for detection at a 1:10,000 dilution.

#### $\alpha$ -Total ERK

Immobilon filters were incubated with an antiserum that recognizes both ERK1 and ERK2 (anti-ERK1-CT, Upstate Biotechnology; 1:1000 to 1:3000), followed by incubation with an HRP-linked goat anti-rabbit IgG antiserum (1:10,000 to 1:30,000).

To prepare for reprobing with a different antibody, we incubated blots at  $50^{\circ}\text{C}$ – $70^{\circ}\text{C}$  in three changes of stripping buffer (62 mM Tris-HCl at pH 6.8, 100 mM  $\beta$ -mercaptoethanol, 2% Sodium Dodecyl Sulfate [SDS]) with occasional agitation, for a total of 1 h. The blots were then washed twice for 10 min with chilled TTBS and placed in the appropriate blocking solution in preparation for the subsequent Western blot.

Densitometric analysis of all immunoreactivities was conducted using a StudioScan desktop scanner and NIH Image software as previously described (English and Sweatt 1996; Atkins et al. 1997). Western blots were developed to be linear in the range used for densitometry.

### ACKNOWLEDGMENTS

Special thanks to James Trzaskos and DuPont Pharmaceuticals for the kind donation of both U0126 and SL327. We thank Richard Paylor for providing us with CD-1 mice and for helpful discussions. We also thank Dan Johnston for critical comments. Funding was

provided by the NIH (grants MH57014 and NS37444) and the NARSAD.

The publication costs of this article were defrayed in part by payment of page charges. This article must therefore be hereby marked "advertisement" in accordance with 18 USC section 1734 solely to indicate this fact.

### REFERENCES

- Adams, J.P., Anderson, A.E., Varga, A.W., Dineley, K.T., Cook, R.G., Pfaffinger, P.J., and Sweatt, J.D. 2000. The A-type potassium channel Kv4.2 is a substrate for the mitogen-activated protein kinase ERK. *J. Neurochem.* **75**: 2277–2287.
- Atkins, C.M., Chen, S.J., Klann, E., and Sweatt, J.D. 1997. Increased phosphorylation of myelin basic protein during hippocampal long-term potentiation. *J. Neurochem.* **68**: 1960–1967.
- Atkins, C.M., Selcher, J.C., Petraitis, J.J., Trzaskos, J.M., and Sweatt, J.D. 1998. The MAPK cascade is required for mammalian associative learning. *Nat. Neurosci.* **1**: 602–609.
- Bland, B.H., Seto, M.G., Sinclair, B.R., and Fraser, S.M. 1984. The pharmacology of hippocampal  $\theta$  cells: Evidence that the sensory processing correlate is cholinergic. *Brain Res.* **299**: 121–131.
- Bliss, T.V.P. and Lomo, T. 1973. Long-lasting potentiation of synaptic transmission in the dentate area of the anaesthetized rabbit following stimulation of the perforant path. *J. Physiol.* **232**: 331–356.
- Chin, J., Angers, A., Cleary, L.J., Eskin, A., and Byrne, J.H. 2002. Transforming growth factor  $\beta$ 1 alters synapsin distribution and modulates synaptic depression in *Aplysia*. *J. Neurosci.* **22**: RC220.
- Coogan, A.N., O'Leary, D.M., and O'Connor, J.J. 1999. P42/44 MAP kinase inhibitor PD98059 attenuates multiple forms of synaptic plasticity in rat dentate gyrus in vitro. *J. Neurophysiol.* **81**: 103–110.
- Costa, R.M., Federov, N.B., Kogan, J.H., Murphy, G.G., Stern, J., Ohno, M., Kucherlapati, R., Jacks, T., and Silva, A.J. 2002. Mechanism for the learning deficits in a mouse model of neurofibromatosis type 1. *Nature* **415**: 526–530.
- Crawley, J.N., Belknap, J.K., Collins, A., Crabbe, J.C., Frankel, W., Henderson, N., Hitzemann, R.J., Maxson, S.C., Miner, L.L., Silva, A.J., et al. 1997. Behavioral phenotypes of inbred mouse strains: Implications and recommendations for molecular studies. *Psychopharmacology (Berl)* **132**: 107–124.
- Crow, T., Xue-Bian, J.-J., Siddiqi, V., Kang, T., and Neary, J.T. 1998. Phosphorylation of mitogen-activated protein kinase by one-trial and multi-trial classical conditioning. *J. Neurosci.* **18**: 3480–3487.
- Davis, S., Vanhoutte, P., Pages, C., Caboche, J., and Laroche, S. 2000. The MAPK/ERK cascade targets both Elk-1 and cAMP response element-binding protein to control long-term potentiation-dependent gene expression in the dentate gyrus in vivo. *J. Neurosci.* **20**: 4563–4572.
- Dudek, S.M. and Fields, R.D. 2001. Mitogen-activated protein kinase/extracellular signal-regulated kinase activation in somatodendritic compartments: Roles of action potentials, frequency, and mode of calcium entry. *J. Neurosci.* **21**: RC122.
- English, J.D. and Sweatt, J.D. 1996. Activation of p42 mitogen-activated protein kinase in hippocampal long term potentiation. *J. Biol. Chem.* **271**: 24329–24332.
- English, J.D. and Sweatt, J.D. 1997. A requirement for the mitogen-activated protein kinase cascade in hippocampal long term potentiation. *J. Biol. Chem.* **272**: 19103–19106.
- Hoffman, D.A., Magee, J.C., Colbert, C.M., and Johnston, D. 1997.  $\text{K}^+$  channel regulation of signal propagation in dendrites of hippocampal pyramidal neurons. *Nature* **387**: 869–875.
- Impey, S., Obrietan, K., Wong, S.T., Poser, S., Yano, S., Wayman, G., Deloume, J.C., Chan, G., and Storm, D.R. 1998. Cross talk between ERK and PKA is required for  $\text{Ca}^{2+}$  stimulation of CREB-dependent transcription and ERK nuclear translocation. *Neuron* **21**: 869–883.
- Jones, M.W., French, P.J., Bliss, T.V., and Rosenblum, K. 1999. Molecular mechanisms of long-term potentiation in the insular cortex in vivo. *J. Neurosci.* **19**: RC36.

- Kanterewicz, B.I., Urban, N.N., McMahon, D.B., Norman, E.D., Giffen, L.J., Favata, M.F., Scherle, P.A., Trzaskos, J.M., Barrionuevo, G., and Klann, E. 2000. The extracellular signal-regulated kinase cascade is required for NMDA receptor-independent LTP in area CA1 but not area CA3 of the hippocampus. *J. Neurosci.* **20**: 3057-3066.
- Larson, J., Wong, D., and Lynch, G. 1986. Patterned stimulation at the  $\theta$  frequency is optimal for the induction of hippocampal long-term potentiation. *Brain Res.* **368**: 347-350.
- Liu, J., Fukunaga, K., Yamamoto, H., Nishi, K., and Miyamoto, E. 1999. Differential roles of  $\text{Ca}^{2+}$ /calmodulin-dependent protein kinase II and mitogen-activated protein kinase activation in hippocampal long-term potentiation. *J. Neurosci.* **19**: 8292-8299.
- Martin, K.C., Michael, D., Rose, J.C., Barad, M., Casadio, A., Zhu, H., and Kandel, E.R. 1997. MAP kinase translocates into the nucleus of the presynaptic cell and is required for long-term facilitation in *Aplysia*. *Neuron* **18**: 899-912.
- Mazzucchelli, C., Vantaggiato, C., Ciamei, A., Fasano, S., Pakhotin, P., Krezel, W., Welzl, H., Wolfer, D.P., Pages, G., Valverde, O., et al. 2002. Knockout of ERK1 MAP kinase enhances synaptic plasticity in the striatum and facilitates striatal-mediated learning and memory. *Neuron* **34**: 807-820.
- Michael, D., Martin, K.C., Seger, R., Ning, M.-M., Baston, R., and Kandel, E.R. 1998. Repeated pulses of serotonin required for long-term facilitation activate mitogen-activated protein kinase in sensory neurons of *Aplysia*. *Proc. Natl. Acad. Sci.* **95**: 1864-1869.
- Nguyen, P.V., Abel, T., Kandel, E.R., and Bourtochouladze, R. 2000. Strain-dependent differences in LTP and hippocampus-dependent memory in inbred mice. *Learn Mem.* **7**: 170-179.
- Norman, E.D., Thiels, E., Barrionuevo, G., and Klann, E. 2000. Long-term depression in the hippocampus in vivo is associated with protein phosphatase-dependent alterations in extracellular signal-regulated kinase. *J. Neurochem.* **74**: 192-198.
- Paylor, R., Baskall-Baldini, L., Yuva, L., and Wehner, J.M. 1996. Developmental differences in place-learning performance between C57BL/6 and DBA/2 mice parallel the ontogeny of hippocampal protein kinase C. *Behav. Neurosci.* **110**: 1415-1425.
- Roberson, E.D., English, J.D., Adams, J.P., Selcher, J.C., Kondratik, C., and Sweatt, J.D. 1999. The mitogen-activated protein kinase cascade couples PKA and PKC to cAMP response element binding protein phosphorylation in area CA1 of hippocampus. *J. Neurosci.* **19**: 4337-4348.
- Rosenblum, K., Futter, M., Jones, M., Hulme, E.C., and Bliss, T.V. 2000. ERK1/II regulation by the muscarinic acetylcholine receptors in neurons. *J. Neurosci.* **20**: 977-985.
- Schmid, R.S., Graff, R.D., Schaller, M.D., Chen, S., Schachner, M., Hemperly, J.J., and Maness, P.F. 1999. NCAM stimulates the Ras-MAPK pathway and CREB phosphorylation in neuronal cells. *J. Neurobiol.* **38**: 542-558.
- Selcher, J.C., Atkins, C.M., Trzaskos, J.M., Paylor, R., and Sweatt, J.D. 1999. A necessity for MAP kinase activation in mammalian spatial learning. *Learn Mem.* **6**: 478-490.
- Selcher, J.C., Nekrasova, T., Paylor, R., Landreth, G.E., and Sweatt, J.D. 2001. Mice lacking the ERK1 isoform of MAP kinase are unimpaired in emotional learning. *Learn Mem.* **8**: 11-19.
- Staubli, U. and Lynch, G. 1987. Stable hippocampal long-term potentiation elicited by ' $\theta$ ' pattern stimulation. *Brain Res.* **435**: 227-234.
- Thomas, M.J., Watabe, A.M., Moody, T.D., Makhinson, M., and O'Dell, T.J. 1998. Postsynaptic complex spike bursting enables the induction of LTP by  $\theta$  frequency synaptic stimulation. *J. Neurosci.* **18**: 7118-7126.
- Watabe, A.M., Zaki, P.A., and O'Dell, T.J. 2000. Coactivation of  $\beta$ -adrenergic and cholinergic receptors enhances the induction of long-term potentiation and synergistically activates mitogen-activated protein kinase in the hippocampal CA1 region. *J. Neurosci.* **20**: 5924-5931.
- Watanabe, S., Hoffman, D.A., Migliore, M., and Johnston, D. 2002. Dendritic  $\text{K}^+$  channels contribute to spike-timing dependent long-term potentiation in hippocampal pyramidal neurons. *Proc. Natl. Acad. Sci.* **99**: 8366-8371.
- Winder, D.G., Martin, K.C., Muzzio, I.A., Rohrer, D., Chruscinski, A., Kobilka, B., and Kandel, E.R. 1999. ERK plays a regulatory role in induction of LTP by  $\theta$  frequency stimulation and its modulation by  $\beta$ -adrenergic receptors. *Neuron* **24**: 715-726.
- Wu, S.P., Lu, K.T., Chang, W.C., and Gean, P.W. 1999. Involvement of mitogen-activated protein kinase in hippocampal long-term potentiation. *J. Biomed. Sci.* **6**: 409-417.
- Yuan, L.L., Adams, J.P., Swank, M., Sweatt, J.D., and Johnston, D. 2002. Protein kinase modulation of dendritic  $\text{K}^+$  channels in hippocampus involves a mitogen-activated protein kinase pathway. *J. Neurosci.* **22**: 4860-4868.

Received June 10, 2002; accepted in revised form November 26, 2002.